Revista de Ciencias Tecnológicas (RECIT). Universidad Autónoma de Baja California ISSN 2594-1925
Volumen 1 (1): 12-22 Julio-Septiembre 2018 https://doi.org/10.37636/recit.v111222.

A feedforward-moment-gyro-control for positioning wirelessly light-source and wireless- camera in laparoscopic instruments

Un control giroscópico de momento de avance para posicionar de forma inalámbrica la fuente de luz y la cámara inalámbrica en instrumentos laparoscópicos

Torres-Ventura José[1], Reyna-Carranza Marco Antonio[1], Rascón-Carmona Raúl[2], Bravo-Zanoguera Miguel Enrique[1], López-Avitia Roberto[1]

[1]Cuerpo Académico de Bioingeniería y Salud Ambiental. Instituto de Ingeniería, Universidad Autónoma de Baja California (UABC), Blvd. Benito Juárez y Calle de la Normal S/N,
Colonia Insurgentes Este C.P. 21280. Mexicali, Baja California, México.

[2]Facultad de Ingeniería de la UABC. Blvd. Benito Juárez y Calle de la Normal S/N, Colonia Insurgentes Este C.P. 21280. Mexicali, Baja California, México.

Corresponding author: Marco Antonio Reyna Carranza, Cuerpo Académico de Bioingeniería y Salud Ambiental. Instituto de Ingeniería, Universidad Autónoma de Baja California (UABC), Blvd. Benito Juárez y Calle de la Normal S/N, Colonia Insurgentes Este C.P. 21280. Mexicali, Baja California, México. E-mail: investigador.reyna@gmail.com. ORCID: 0000-0001-9954-2958.

Recibido: 05 de Junio del 2017 **Aceptado:** 03 de Febrero del 2018 **Publicado:** 26 de Septiembre del 2018

Resumen. - *En este artículo se presenta un sistema mecatrónico giroscópico, que ayuda al cirujano laparoscópico a controlar de forma inalámbrica el zoom y la posición panorámica de una cámara y una fuente de luz, adaptadas a un manipulador para cirugía mínimamente invasiva. El giroscopio adaptado al manipulador, genera una señal de referencia utilizada por un control de lazo abierto. El sistema de cámara y fuente de luz, está montado sobre un dispositivo electromecánico (brazo robótico) de tres grados de libertad (3DOF). El éxito se mide haciendo una comparación de una señal de entrada a partir de los niveles de voltaje generados por un transductor con tecnología de sistemas micro-electro-mecánicos (MEMS), versus las señales para las posiciones angulares de dos servomotores (trayectoria panorámica e inclinación) y el acercamiento o alejamiento de la cámara por un motor DC.*

Palabras clave: Mínimamente Invasivo; Robot Cirujano; Adquisición de Datos; Control de Giro de Momento de Avance; Transceptor Inalámbrico; Laparoscopía.

Abstract. - *This article presents a gyroscopic mechatronic system, which helps the laparoscopic surgeon to wirelessly control the zoom and panoramic position of a camera and a light source, adapted to a manipulator for minimally invasive surgery. The gyroscope adapted to the manipulator generates a reference signal used by an open loop control. The camera and light source system are mounted on an electromechanical device (robotic arm) with three degrees of freedom (3DOF). Experiments performed with the system show good pan, tilt and zoom performance of the camera and light source. Success is measured by comparing an input signal from the voltage levels generated by a transducer with micro-electro-mechanical systems (MEMS), versus the signals for the angular positions of two servo-motors (pan and tilt) and zooming in or out of the camera by a DC motor.*

Keywords: Minimally Invasive; Robot Surgeon; Data Acquisition; Feedforward-Moment-Gyro-Control; Wireless Transceiver; Laparoscopy.

ISSN: 2594-1925

1. Introduction

Mechatronics has actively participated in the rehabilitation of patients in about 10 % of the total world population according to the World Health Organization (WHO) [1−3].

One of the elements widely used in medical applications is transducers [4, 5], which are proposed to support surgeons in the laparoscopic field. An important topic addressed by this field is to move a laparoscopic camera and light into the abdominal cavity; the camera provides continuous video images taken from the pelvic abdominal cavity of the patient. Nowadays, the position control of camera and light is achieved by using vision, voice and mechanical interfaces. Some solutions to manipulate position in this kind of instruments came from mechatronics assistance with three degrees of freedom (PMAT) [6], where a mechanical harness is placed over the shoulders of the surgeon and provides the position for the camera view. Another system is the robotic camera assistant (EndoAssist) [7], where the surgeon moves the laparoscopic camera through a helmet equipped with an infrared light emitting diode (IR LED) transmitter, which is in contact with an LED receiver placed on a remote monitor. This system allows changing the angle of a camera placed inside the pelvic cavity of the patient.

Other methods, like those used in the automated endoscopic system for the optimal position (AESOP) and the KAIST laparoscopic assistant robot systems (KALAR), use voice commands issued by the surgeon [8, 9].

Another alternative used is the single port access (SPA) [10], which consists of making a hole of 26 *mm* of diameter below the navel through which an independent camera is introduced and then controlled from the outside by an electromagnetic field [11].

Another minimally invasive surgical robot is the insertable robotic effector's platform (IREP) [12], which is a wire-actuated wrist with a passive flexible component arm that is introduced to manipulate the trajectory of the laparoscopic camera and light [13]. Finally, the robotic cameraman is an industrial robotic arm, whose end tip was adapted to provide video images as it moves into the abdominal cavity of a patient [14].

This paper presents a prototype mechatronic system (i.e. a feedforward-moment-gyro-control) to move wirelessly a laparoscopic wireless-camera and light-source inside the abdominal cavity of a patient [15, 16].

2. Methodology

2.1. Principles of the system

A feedforward-control is implemented to achieve the reference position of the camera; this reference signal is given by an electronic gyroscope mounted on a laparoscopic grasper instrument. The surgeon decides when to start or stop this task by pressing with the thumb a force sensor (FSR) installed in the instrument (i.e. grasper of 5 *mm* of diameter).

The mechanical prototype is supported on transducer technology of micro-electro-mechanical systems (MEMS), which involves a conversion of energy into a voltage. Moreover, the output of the angular rate sensor (i.e. gyroscope) is amplified and used as a reference signal to move the camera on three different axes: pan, tilt (both are rotational) and zoom (translational).
The gyroscope has a sensitivity of 300 $mV/°/s$ as reported by their manufacturers. Some of these control applications in the medical field can be consulted in [17, 18]. Concerning the issue of security related to radiate power levels for medical instruments in the operating room, there are some previous works that give some recommendations [19–22].

As shown in Figure 1, the process begins when the surgeon presses with the thumb the FSR (Mod. FSR 402). If the surgeon does not press the FSR, the laparoscopic instrument (i.e. the master manipulator) is used as an instrument of standard surgery.

ISSN: 2594-1925

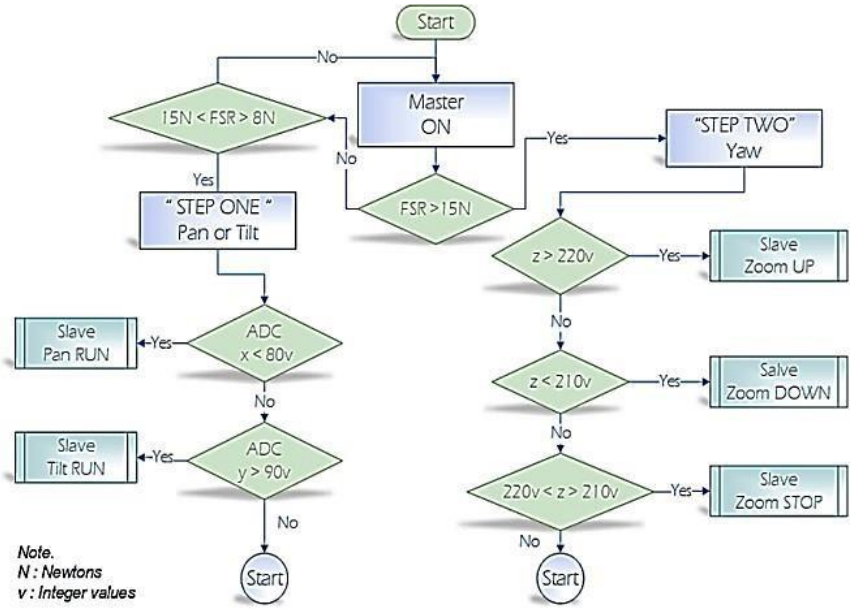

Figure 1. Master/slave feedforward control process to position laparoscopic camera and light.

2.2. Laparoscopic vision system

Figure 2 represents in blocks: (1) transceiver [23] gyroscope board (ADXL335), which is mounted on a laparoscopic instrument (disposable monopolar scissor, 17 *mm* blade); (2) 3DOF robotic arm, which is composed by a control board (ATmega2560), two servomotors (SA-1283SG), and one gear motor (MTS50-Z8); (3) wireless white-light mini-camera (type: pin hold lens, 12 volts, 2.4 *GHz*, 628 x 582 pixels) mounted on the tip of a laparoscopic instrument (type: 5 *mm* needle driver, Mod. Da Vinci 400117 Endowrist instrument) as shown in Figures 3 and 4; and (4) Liquid Crystal Display (LCD) monitor (Mod: 32" HD Plano TV FH4005 Series 4) with wireless video input (AV-IN) for reception of images that come from the wireless laparoscopic camera. The images are transmitted from the laparoscopic camera to the LCD monitor using the radio frequency (RF) channel 2 at 2.49 *GHz*. The laparoscopic instrument (master manipulator) communicates with the 3DOF robotic arm (slave manipulator) using the standard IEEE 802.15.4 [24 – 26] by the RF channel 1 at 2.68 *GHz*.

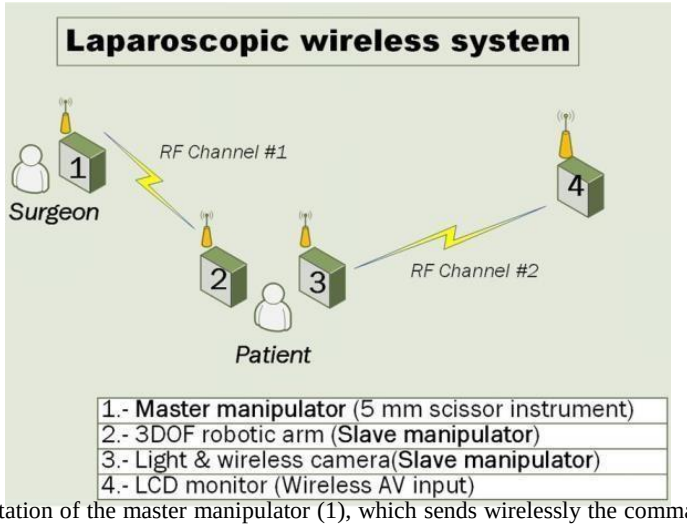

Figure 2. The surgeon controls the orientation of the master manipulator (1), which sends wirelessly the commands to the robotic arm (2) via the RF channel 1; at the same time the wireless-camera (3), which is inside the patient, sends the video images to the LCD monitor (4) via the RF channel 2.

ISSN: 2594-1925

2.3. Laparoscopic master manipulator

Figure 3 shows a traditional laparoscopic instrument (5 *mm* scissor), which was modified by adding a gyroscope on it.

When the instrument rotates, the transducer detects the angle of motion and converts it into a voltage signal command, as shown in Figure 4.

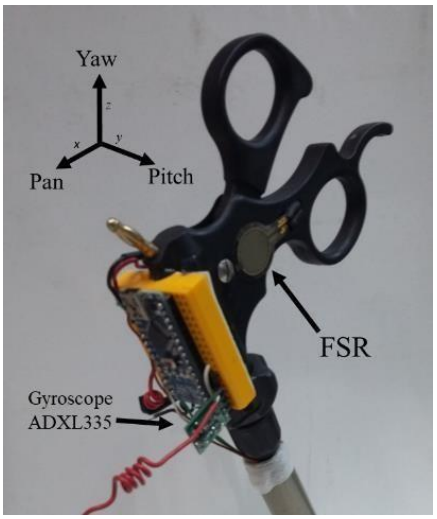

Figure 3. The master manipulator was modified to insert an FSR. The surgeon can press using the thumb to start or stop the remote position of the trajectory of the laparoscopic wireless-camera.

2.4. Slave manipulator dynamic model

Given that the manipulator of 3DOF is represented by the rectilinear motion $q_1 \in \mathbb{R}$ and 2 angular motions $q_2 \in \mathbb{R}$, $q_3 \in \mathbb{R}$, where q_1 stands for the zoom, q_2 is the tilt displacement and q_3 is the pan displacement as depicted in Figure 5, according to the modelling procedure of the Lagrange equations of motion [27]. Firstly, let us compute the kinetic energy of the manipulator, which is given by:

$$k(q, \dot{q}) = \tfrac{1}{2} [m_1 \dot{q_1} + m_2 \dot{q_2} + m_3 \dot{q_3}] \qquad (1)$$

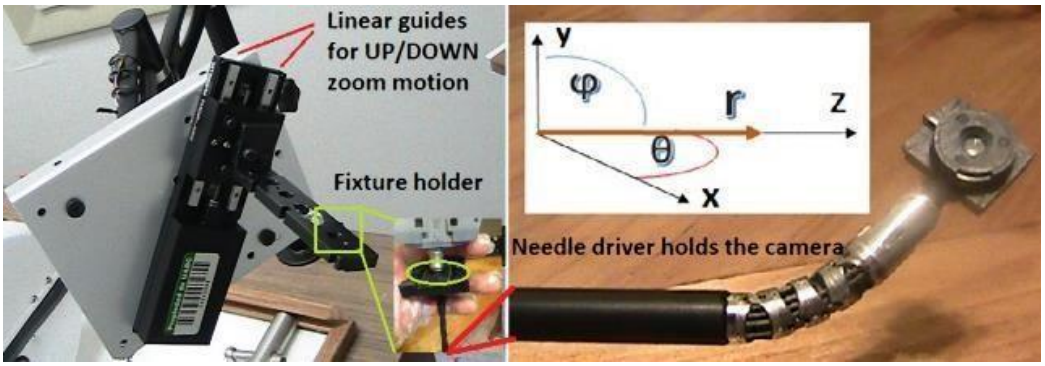

Figure 4. A 3DOF mechanical arm (left). The spherical coordinate system was introduced to better illustrate the motion of pan, tilt, and zoom within the abdomen of the patient. It is not necessary any conversion between coordinate systems (right).

ISSN: 2594-1925

Moreover, the manipulator is not affected by gravity, therefore the potential energy is:

$$U(q) = 0 \quad (2)$$

From eq. (1) and (2) we can compute the Lagrangian

$$L(q, \dot{q}) = K(q, \dot{q}) - U(q)$$

$$= \tfrac{1}{2}[m_1\dot{q}_1 + m_2\dot{q}_2 + \dot{q}_3] \quad (3)$$ We have that

$$\partial L/(\partial q_1) = \partial L/(\partial q_2) = \partial L/(\partial q_3) = 0$$

$$\partial L/(\partial \dot{q}_1) = m_1\dot{q}_1$$

$$\partial L/(\partial \dot{q}_2) = m_2\dot{q}_2$$

$$\partial L/(\partial \dot{q}_3) = m_3\dot{q}_3$$

$$d/dt\,[\partial L/(\partial \dot{q}_1)] = m_1\ddot{q}_1$$

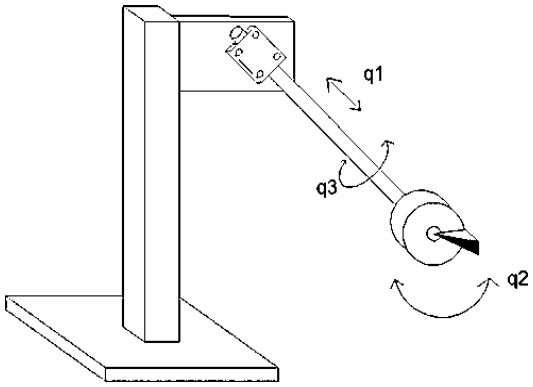

Figure 5. The slave manipulator: 3DOF robotic arm with a camera on the end effector.

$$d/dt\,[\partial L/(\partial \dot{q}_2)] = m_1\ddot{q}_2 d/dt\,[\partial L/(\partial \dot{q}_3)] = m_1\ddot{q}_3$$

The Lagrange equations of motion for the manipulator are given by:

$$d/dt\,[\partial L(q,\dot{q})/(\partial \dot{q})] - \partial L(q,\dot{q})/\partial q = \tau \quad (4)$$

where $q = [q_1\ q_2\ q_3]^T \in \mathbb{R}^3$ and the control input is $\tau = [\tau_1\ \tau_2\ \tau_3]^T \in \mathbb{R}^3$, or equivalently

$$d/dx\,[\partial L(q,\dot{q})/(\partial \dot{q}_i)] - \partial L(q,\dot{q})/(\partial q_i) = \tau_i, \quad i = 1, 2, 3. \quad (5)$$

The dynamic model of the system in joint space coordinates is as follows:

$$d/dt\,[\begin{matrix} q \\ \dot{q} \end{matrix}] = [\begin{matrix} \dot{q} \\ \tau/m \end{matrix}] \quad (6)$$

with $q = [q_1, q_2, q_3]^T \in \mathbb{R}^3$, $\tau = [\tau_1, \tau_2, \tau_3]^T \in \mathbb{R}^3$ and $[m_1, m_2, m_3]^T \in \mathbb{R}^3$, we will have an infinite number of equilibrium points:

$$[q_1\ q_2\ q_3\ \dot{q}_1\ \dot{q}_2\ \dot{q}_3]^T = [S_1\ S_2\ S_3\ 0\ 0\ 0]^T$$

Being $S_1 = q_1(0)$, $S_2 = q_2(0)$, $S_3 = q_3(0) \in \mathbb{R}$, the control input $\tau \in \mathbb{R}^3$ is given by the gyroscope and the strain gauge mounted on the laparoscopic

ISSN: 2594-1925

grasper as is shown in Figure 3.

2.5. *Feedforward control*

The surgeon, when using the master manipulator instrument, would have a limited working space due to the wrist of the hand plus the small dimension of the 5-mm diameter hole of the patient. Hence, the rotation over coordinates *x*, *y* and *z* are restricted from 0 to 90 degrees for each axis (-α to α, -β to β, and -θ to θ respectively). Furthermore, the slave manipulator (i.e. laparoscopic wireless-camera) has a working space in spherical coordinates restricted from 0 to 90 (-φ to φ, -θ to θ) as depicted in Figure 3; the differences and restrictions are shown in Table 1A. The relationship between the *z* axis in the Cartesian system and the *r* axis in the Spherical system is shown in Table 1B.

Table 1. Relationship of the Cartesian and Spherical system: (A) Pan and tilt trajectory. (B) Zoom trajectory.

A

Master Manipulator (5mm scissors)				Slave manipulator (needle driver)		
Direction (Axes)	Displacement (Radians)	Orientation (Spinning)	Position (Degrees)	Angle	Position (Degrees)	Camera (Direction)
x (roll)	q_2	Turn right	0 to 45	φ	0 to 45	Pan to right side
x (roll)	$-q_2$	Turn left	0 to -45	$-\varphi$	0 to -45	Pan to left side
y (pitch)	q_3	Turn right	0 to 45	θ	0 to 45	Tilt to right side
y (pitch)	$-q_3$	Turn left	0 to -45	$-\theta$	0 to -45	Tilt to left side

B

Master Manipulator (5mm scissors)				Slave manipulator (needle driver)		
Direction (Axis)	Displacement (*mm*)	Orientation (spinning)	Position (degrees)	Axis	Position (*mm*)	Camera (direction)
z (yaw)	q_1	Turn right	0 to 45	*r*	0 to 50	Zoom up
z (yaw)	$-q_1$	Turn left	0 to -45	*r*	50 to 0	Zoom down

Table 2. Encoding structure to position servomotors on the 3DOF robotic arm.

Master manipulator					Slave manipulator
Gyroscope (Axes orientation)	Orientation (Degrees)	Encoding data (Integer value)	FSR (Step)	Command (Direction)	Position (Degrees)
x (roll)	-45 to 45	0 to 80	One	Pan	-45 to 45
y (pitch)	-45 to 45	90 to 170	One	Tilt	-45 to 45

Table 3. Encoding structure to position the dc gear motor on the 3DOF robotic arm

Master manipulator					Slave manipulator
Gyroscope (Axis orientation)	Orientation (Degrees)	Encoding data (Integer value)	FSR (Step)	Command (Direction)	Position (Logic state)
z	45 to 25	180 to 210	Two	Zoom down	ON
z	-45 to -25	221 to 254	Two	Zoom up	ON
z	-24 to 24	211 to 220	Two	Stop	OFF

2.6. *Master manipulator board*

The gyroscope was adjusted to measure the orientation around the *x*-axis from -45 to 45 degrees, around the *y*-axis from -45 to 45 degrees and around the *z*-axis from 45 to -45. An algorithm was developed to position the wireless-camera and light considering protocol shown in Table 2 and Table 3.

2.7. *Data acquisition system for master manipulator*

To assess the matches of the position of laparoscopic wireless-camera and light versus the orientation of the gyroscope, we collected the proportional output voltage from the *x*, *y*, and *z*-axes of the gyroscope and converted this into a digital signal with a

ISSN: 2594-1925

microcontroller [28]. The ATmega326 supports 10 *bits* of resolution and was adjusted to 3.3 *V* as a reference voltage. Therefore, 3.29 *V* (LSB * 1023) is, in theory, the maximum voltage available. Thus, the error can be expressed as 0.097 *%* (0.00323 *V* * 100 / 3.3 *V*).

3. Results

Figure 6 shows how the trajectory position of the servomotor is controlled. These results are representative for both angular displacements q_2 and q_3, but only one (pan) is reported.

3.1. Servomotor rotation degrees for pan and tilt

The servomotors that control the movement of pan and tilt properly do not have an encoder, so a mechanism was adapted to take the readings, using an incremental type DC encoder with resolution of 100 *rpm* at 5 *V*. In the same way in Figure 6 it is observed that the operating voltage of the *x*-axis of the gyroscope lies within the limits of the aforesaid theoretical voltage.

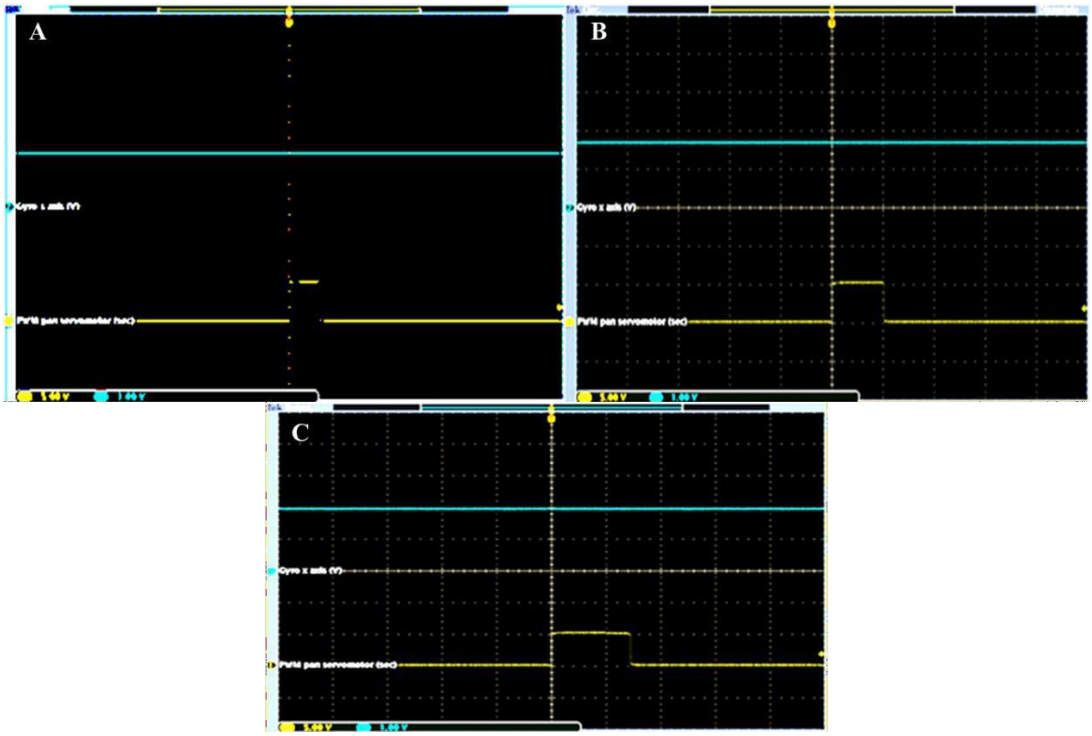

Figure 6. (A) Upper line is the voltage level from gyroscope output (1.4 *V*). The lower line is the pulse width (0.6 *ms*) at the ADC output, which positions the servomotor on the -13 degrees. (B) The upper line is the voltage level from gyroscope output (1.0 *V*). The lower line is the pulse width (1.0 *ms*) at the ADC output, which positions the servomotor on the 13 degrees. (C) The upper line is the voltage level from gyroscope output (1.98 *V*). The lower line is the pulse width (1.5 *ms*) at the ADC output, which positions the servomotor on the 42 degrees.

3.2. The zoom trajectory from DC gear motor

The data logger records the voltage signal around the *z*-axis. Figure 7 shows that when the orientation of the gyroscope is less than 75 degrees, the zoom is moving down; when the gyroscope is greater than 125 degrees, the zoom is moving up; and when the gyroscope rotates between 76 and 124 degrees, the zoom is stopping.

The rectilinear motion q_1 zooms the laparoscopic wireless-camera.

ISSN: 2594-1925

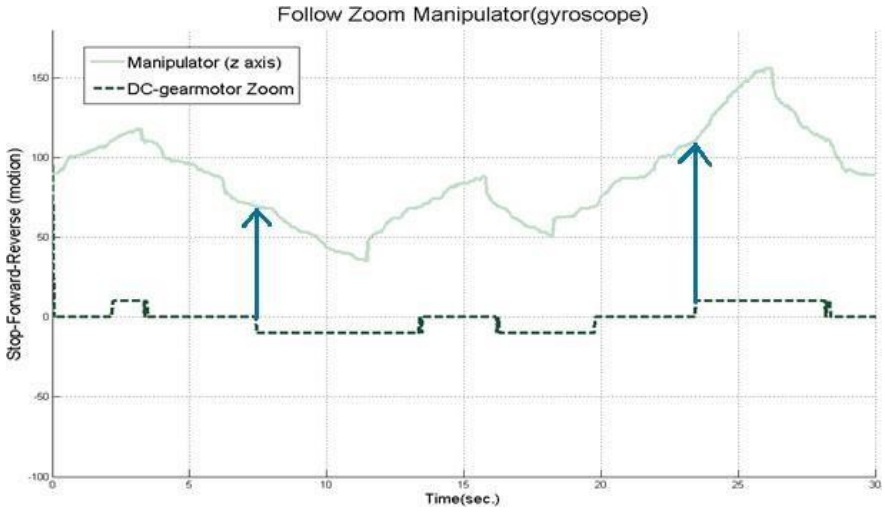

Figure 7. Data logging for reference tracking using the linear motor MTS50-Z8, which was used for the zooming motion.

4. Discussion

According to the results obtained by the DAQ system to assess the position of the laparoscopic camera and light, we analyzed and displayed the error through the process of conversion by the ADC system as shown in Figure 8. For instance, for a voltage of 1.98 *V* in the *x*-axis of the gyroscope, we had a response of 45° in the servomotor.

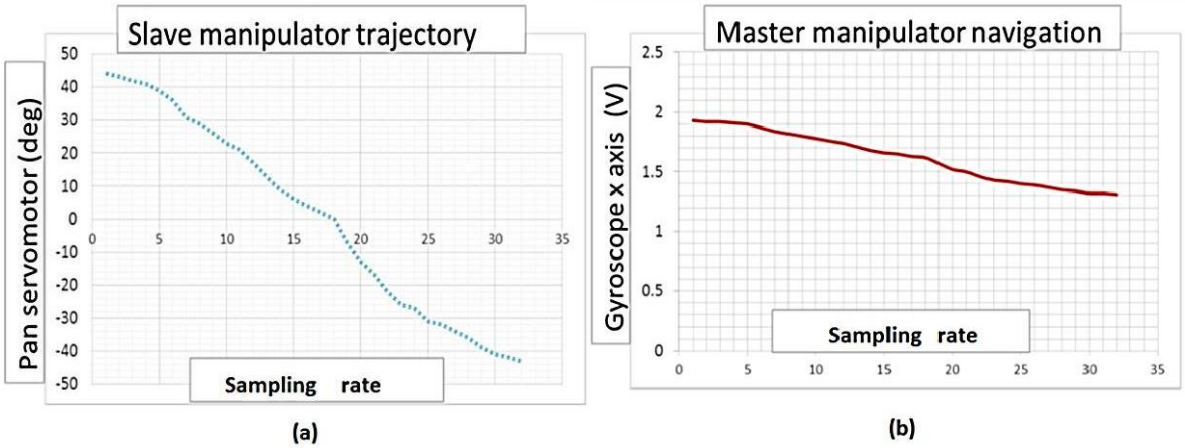

Figure 8. (a) Data logger for the response of servomotor rotation degree, the vertical axis is the position in degrees; it can be seen how it decreases as sampling rate increases. (b) The gyroscope *x*-axis output signal, it can be observed that the voltage corresponding to the *x*-axis decreases as the sampling rate increases.

The present study showed that the position of a laparoscopic camera and light (slave manipulator) inside the abdomen of a patient can be controlled by the surgeon with a laparoscopic instrument (master manipulator). Also, showed that 300 $mV/°/s$ of gyroscope sensitivity is enough to guide the pan and tilt view of the camera and light. Considering that at lower sensitivity we get lower resolution, we will estimate with Eq. 7 the absolute error and with Eq. 8 the scientific error.

$$\sum^{n} |xi-\bar{X}$$

communication by the module RF NRF24L01 does not affect the response of the gear dc motor and the servomotor, due to the fact that this signal is used as a reference for both actuators.

$$e = \frac{i=1}{N} \quad (7)$$

ISSN: 2594-1925

5. Conclusion

Where: $X = \bar{X} \pm e$ (8)

x_i = Sensitivity $mV/°/s$
$\bar{X}$ = Mean.
n = Total Reading.
X = Scientific Error.

In this way, the absolute error e = 0.20 is estimated;

In this work, it was shown that a surgeon can modify the trajectory of a laparoscopic camera and

which represented in terms of scientific error has an error in the range of 1,089 – 1,289, which represents a degree of positive sensitivity. The behavior of the experiment is shown in Figure 9.

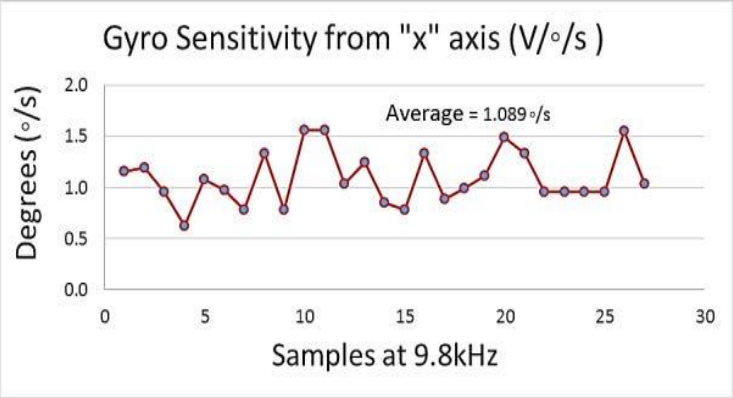

Figure 9. Readings were taken by the DAQ as a function of the proportional voltage of the *x*-axis in degrees.

In addition, the results of the experiments show that when entering an FSR sensor to select between two different steps that represent two different spatial planes (with x and y coordinates), we can send information in the first step to the servomotors for pan and tilt motion, and the second step to send information to gear dc motor for the zoom motion.

Finally, the accuracy of the digitizing process of the output voltage for the *x*-axis of the gyroscope, versus the response of the electromechanical actuators (servomotors and gear motor), was demonstrated by the data record that represents the output voltage at the microcontroller AT mega328. The signal sent through the path of wireless light using a laparoscopic instrument with an embedded board containing a gyroscope. The surgeon decides when to move the laparoscopic camera in three axes (pan, tilt, and zoom). The three axes can move back and forward. Although a feedforward control system cannot correct the errors that could be generated, nor compensate the perturbations affecting the system, nonetheless, some advantages of using this type of control are its simplicity of implementation and low cost.

Acknowledgments

Thanks to Universidad Autónoma de Baja California and CONACYT for the support of this work.

ISSN: 2594-1925

References

[1] Meng W, Liu Q, Zhou Z, Ai Q, Sheng B, & Xie SS. "Recent development of mechanisms and control strategies for robot- assisted lower limb rehabilitation," *Mechatronics.* 31:132- 145, 2015. https://doi.org/10.1016/j.mechatronics.2015.04.005

[2] Ouyang X, Ding S, Fan B, Li PY, & Yang H. "Development of a novel compact hydraulic power unit for the exoskeleton robot," *Mechatronics*. 38: 68-75, 2016. https://doi.org/10.1016/j.mechatronics.2016.06.003

[3] Wu J, Gao J, Song R, Li R, Jiang L. "The design and control of a 3DOF lower limb rehabilitation robot," *Mechatronics*, vol. 33, pp. 13-22, 2016. https://doi.org/10.1016/j.mechatronics.2015.11.010

[4] Blanes C, Mellado M, Beltrán P. "Tactile sensing with accelerometers in prehensile grippers for robots," *Mechatronics*, vol. 33, pp. 1-12, 2016. https://doi.org/10.1016/j.mechatronics.2015.11.007

[5] Abir J, Longo S, Morantz P, Shore P. "Optimized estimator for real-time dynamic displacement measurement using accelerometers." *Mechatronics*, vol.39, pp.1- 11, 2016. https://doi.org/10.1016/j.mechatronics.2016.07.003

[6] Mishra R, Lorias D, Minor A. "Comparison of PMAT camera holder with human camera holder," World Journal of Laparoscopic, vol. 1, no. 2, pp. 1-5, 2008. https://doi.org/10.5005/jp-journals-10007-1049

[7] Wagner A, Varkarakis I, Link R, Sullivan W, Su L. "Comparison of surgical performance during laparoscopic radical prostatectomy of two robotic camera holders," *EndoAssist and AESOP; a pilot study*, vol. 68, no. 1, pp. 70-74, 2006. *https://doi.org/10.1016/j.urology.2006.02.003*

[8] Pugin F, Bucher P, Morel P. "History of robotic surgery: from AESOP and Zeus to da Vinci," *Journal of visceral surgery*, vol. 148, no. 5, pp. 3-8, 2011. https://doi.org/10.1016/j.jviscsurg.2011.04.007

[9] Kim J, Lee Y, Ko S, Kwon D. "Compact camera assistant robot for minimally invasive surgery: KaLAR," in Proc. IEEE/RSJ International Conference, 2004, pp. 2587-2592. https://doi.org/10.1109/IROS.2004.1389798.

[10] Pugin F, Bucher P, Morel P. "History of robotic surgery. AESOP and Zeus to da Vinci," *Journal of visceral surgery*, vol. 148, no. 5, pp. 3-8, 2011. https://doi.org/10.1016/j.jviscsurg.2011.04.007

[11] Liu X, Mancini G, Tan J. "Design and analysis of a magnetic actuated capsule camera robot for single incision laparoscopic surgery," in *Proc. IEEE/RSJ International Conference*, 2015, pp. 229-234. https://doi.org/10.1109/IROS.2015.7353379

[12] Bajo A, Goldman R, Wang L. "Integration and preliminary evaluation of an insertable robotic effectors platform for single port access surgery," in *Proc. IEEE International Conference*, 2012, pp. 3381-2287. https://doi.org/10.1109/ICRA.2012.6224986

[13] Luo R, Wang J, Tsai J, Lee K. "Robotic Flexible Laparoscope with position retrieving system for assistive minimally invasive surgery," IEEE/RSJ International Conference, 2015, pp. 2014-2029. https://doi.org/10.1109/IROS.2015.7353645

[14] Hurteau R, DeSantis S, Begin E. "Laparoscopic surgery assisted by a robotic cameraman: concept and experimental results," in *Proc. IEEE International Conference Robotics and Automation*, 1994, pp. 2286-2289. https://doi.org/10.1109/ROBOT.1994.350945

[15] Yoshida M, Furukawa T, Morikawa Y, Kitagawa Y. "The developments and achievements of endoscopic surgery, robotic surgery and function-preserving surgery," *Japanese Journal of clinical oncology*, vol. 40, no. 9, pp. 863-869, 2010. https://doi.org/10.1093/jjco/hyq138

[16] García O, Olvera H, Beltrán J. "Telemedicina y cirugía robótica en ginecología," *Ginecol Obstet Mex*, vol. 76, no. 3, pp. 161-166, 2008. https://www.medigraphic.com/cgi-bin/new/resumen.cgi?IDARTICULO=19397

[17] Cavusoglu M. "Intelligent control algorithms for robotic- assisted beating heart surgery," *Robotics*, vol. 23, no. 3, pp. 468-480, 2007. https://doi.org/10.1109/TRO.2007.895077

[18] Feng Y, Fuentes D. "Model-based planning and real-time predictive control for laser-induced thermal therapy," *International Journal of Hyperthermia*, vol. 27, no. 8, pp.751- 761, 2011. https://doi.org/10.3109/02656736.2011.611962

[19] Ardavan M, Schmitt K. "A preliminary assessment of EMI control policies in hospitals," in *Proc. Antenna Technology and Applied Electromagnetics*, 2010, pp.1-6. https://doi.org/10.1109/ANTEM.2010.5552553

[20] Tan K, Hinberg I. "Radiofrequency susceptibility tests on medical equipment," in Proc. 16th Annual International Conference of the IEEE, 1994, pp. 998-999. https://doi.org/10.1109/IEMBS.1994.415252

[21] Van Der Togt R, Van Lieshout EJ, Hensbroek R, Beinat E, Binnekade JM, Bakker PJM. "Electromagnetic interference from radio frequency identification inducing potentially hazardous incidents in critical care medical equipment," *Jama*, vol. 299 no. 24, pp. 2884- 2890, 2008. https://doi.org/10.1001/jama.299.24.2884

[22] Chang M, Cheng C, Huang H. "Wireless multi-channel near-infrared spectroscopy for monitoring middle cerebral artery occlusion," *IEEE/SICE International Symposium System Integration*, 2011, pp. 1072-1077. https://doi.org/10.1109/SII.2011.6147598

[23] Cavusoglu M, Rotella J, Newman W. "Control algorithms for active relative motion cancelling for robotic assisted off-pump coronary artery bypass graft surgery," in *Proc. 12th International Conference*, 2005, pp. 431-436. https://doi.org/10.1109/ICAR.2005.1507446

[24] Ting K, Ee G, Ng C, Noordin N. "The performance evaluation of IEEE 802.11 against IEEE 802.15. 4 with low transmission power," in *Proc. 17th Asia-Pacific Conference Communication*, 2011, pp. 850-855. https://doi.org/10.1109/APCC.2011.6152927

[25] Chen CH, Chang H, Liu TP, Huang CH. "Application of wireless electrical non- fiberoptic endoscope: Potential

ISSN: 2594-1925

benefit and limitation in endoscopic surgery," *International Journal of Surgery*, vol. 19, pp. 6-10, 2015. https://doi.org/10.1016/j.ijsu.2015.05.003

[26] Periyasamy M, Dhanasekaran R. "Electromagnetic interference on critical medical equipments by RFID system," in *Proc. Communications and Signal Processing (ICCSP)*, 2013, pp. 668-672. https://doi.org/10.1109/iccsp.2013.6577139

[27] Agrawal OP. "Formulation of Euler–Lagrange equations for fractional variational problems" *Journal of Mathematical Analysis and Applications*, vol. 272, no. 1, pp. 368-379, 2002. https://doi.org/10.1016/S0022-247X(02)00180-4

[28] Carlos J. *"Adquisición de datos con Arduino I: Tiempo de muestreo y Resolución"*: https://booleanbite.com/web/adquisicion-de-datos-con-arduino-i-tiempo-de-muestreo-y-resolucion/ 2015 [Mar. 18, 2015].

ISSN: 2594-1925